

Robust Chaos

Soumitro Banerjee ^{1,*}, James A. Yorke ^{2,†} and Celso Grebogi ^{2,‡}

¹ *Department of Electrical Engineering, Indian Institute of Technology, Kharagpur-721302, India*

² *Institute of Physical Science & Technology, University of Maryland, College Park, MD 20742, USA*

Practical applications of chaos require the chaotic orbit to be robust, defined by the absence of periodic windows and coexisting attractors in some neighborhood of the parameter space. We show that robust chaos can occur in piecewise smooth systems and obtain the conditions of its occurrence. We illustrate this phenomenon with a practical example from electrical engineering.

It has been proposed to make practical use of chaos in communication [1], in enhancing mixing in chemical processes [2] and in spreading the spectrum of switch-mode power supplies to avoid electromagnetic interference [3, 4]. In such applications it will be necessary to obtain reliable operation in the chaotic mode.

It is known that for most smooth chaotic systems (take the logistic map [5] for example), there is a dense set of periodic windows for any range of parameter values. Therefore in practical systems working in chaotic mode, slight inadvertent fluctuation of a parameter may take the system out of chaos. The question is, how to guarantee that there is no periodic window for a given range of parameter values and the maximal Lyapunov exponent remains positive throughout the range? In this Letter, we address this problem.

We say a chaotic attractor is *robust* if, for its parameter values there exists a neighborhood in the parameter space with no periodic attractor and the chaotic attractor is unique in that neighborhood. It is known that robust chaos cannot occur in smooth systems. In this Letter we show that such situations can occur in piecewise smooth maps and obtain the conditions of existence of robust chaos.

We first give a practical example from electrical engineering to demonstrate robust chaos. The circuit shown in Fig.1 is known as the boost converter. It consists of a controlled switch S , an uncontrolled switch D , an inductor L , a capacitor C and a load resistor R . When the controlled switch is turned on, the current in the inductor increases and energy is stored in it. When the controlled switch is turned off, the stored energy in the inductor drops and the polarity of the inductor voltage changes so that it adds to the input voltage. The voltage across the inductor and the input voltage together “boosts” the output voltage to a value higher than the input voltage. Such circuits are widely used in regulated dc switch-mode power supplies.

Regulation of the output current is achieved by controlling the switching by current feedback — known as

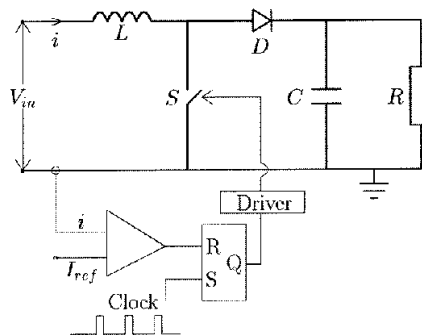


Figure 1: The current mode controlled boost converter

“current-mode control”. In this control logic, the switch is turned on by clock pulses that are spaced T seconds apart. When the switch is closed, the inductor current increases till it reaches the specified reference value I_{ref} . The switch opens when $i = I_{ref}$. Any clock pulse arriving during the *on* period is ignored. Once the switch has opened, the next clock pulse causes it to close.

We obtain a discrete-time model by observing the state variables at every clock instant. There are two ways in which a state can evolve from one clock instant to the next. If the on-time $T_{on} = L(I_{ref} - i_n)/V_{in}$ is less than T , the evolution between observation instants includes one *on* period and one *off* period. Since the clock period typically is much smaller than the characteristic time of the LCR circuit, we assume the waveforms to be linear between clock instants. By neglecting the higher order Taylor terms, the two dimensional map for $T_{on} < T$ is derived as:

$$i_{n+1} = I_{ref} + \frac{1}{L} \left(V_{in} - v_n + \frac{v_n T_{on}}{CR} \right) (T - T_{on})$$

$$v_{n+1} = v_n - \frac{v_n T_{on}}{CR} + \left(\frac{I_{ref}}{C} - \frac{v_n}{CR} + \frac{v_n T_{on}}{C^2 R^2} \right) (T - T_{on})$$

On the other hand, if the clock pulse arrives while $i < I_{ref}$, the switch remains *on* between the observation

instants. If $T_{on} \geq T$, then the map takes the form

$$\begin{aligned} i_{n+1} &= i_n + \frac{V_{in}T}{L} \\ v_{n+1} &= v_n - \frac{v_n}{CR}T \end{aligned}$$

The borderline between the two cases is given by the case where the current reaches I_{ref} exactly at the arrival of the next clock pulse, i.e., $I_{border} = I_{ref} - V_{in}T/L$. The resulting map, therefore, is piecewise smooth.

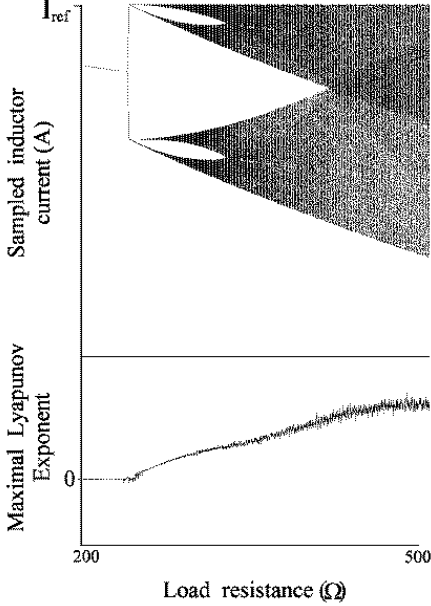


Figure 2: The bifurcation diagram and the Lyapunov spectrum of the boost converter. The parameter values are: $c = 220\mu F$, $I_{ref} = 0.5A$, $V_{in} = 30V$, $T = 400\mu s$, $L = 0.1H$

The bifurcation diagram and the Lyapunov spectrum of the boost converter is presented in Fig.2. It may be noted that there is no periodic window or coexisting attractor in the parameter range $R = [241, 500]\Omega$. The chaotic attractor therefore satisfies the conditions of robustness.

We now obtain the general conditions of occurrence of robust chaos. Let $f(\hat{x}, \hat{y}; \rho)$ be a two-dimensional piecewise smooth map which depends on a single parameter ρ . Let Γ_ρ , given by $\hat{x} = h(\hat{y}, \rho)$ denote a smooth curve that divides the phase plane into two regions R_a and R_b . The map is given by

$$f(\hat{x}, \hat{y}; \rho) = \begin{cases} f_1(\hat{x}, \hat{y}; \rho) & \text{for } \hat{x}, \hat{y} \in R_a, \\ f_2(\hat{x}, \hat{y}; \rho) & \text{for } \hat{x}, \hat{y} \in R_b \end{cases} \quad (1)$$

It is assumed that the functions f_1 and f_2 are both continuous and have continuous derivatives. The map f is continuous but its derivative is discontinuous at the line Γ_ρ , called the ‘‘border’’. It is further assumed that the one-sided partial derivatives at the border are finite. We

study the bifurcations of this system as the parameter ρ is varied.

If a bifurcation occurs when the fixed point of the map is in one of the smooth regions R_a or R_b , it will be one of the ‘‘standard’’ types, namely period doubling, saddle-node or Hopf bifurcation. But if the bifurcation occurs when the fixed point is *on* the border, there is a discontinuous change in the elements of the Jacobian matrix as ρ is varied. A rich variety of bifurcations have been reported [6, 7, 8] in this situation, which have been called border collision bifurcation. We show that under certain conditions border collision bifurcation results in robust chaos.

It has been shown [6] that by a change of coordinates, any piecewise smooth map can be reduced to the normal form (2) in some small neighborhood of the fixed point undergoing border collision bifurcation.

$$G_\mu = \begin{cases} \begin{pmatrix} \tau_L & 1 \\ -\delta_L & 0 \end{pmatrix} \begin{pmatrix} x \\ y \end{pmatrix} + \mu \begin{pmatrix} 1 \\ 0 \end{pmatrix}, & \text{for } x \leq 0, \\ \begin{pmatrix} \tau_R & 1 \\ -\delta_R & 0 \end{pmatrix} \begin{pmatrix} x \\ y \end{pmatrix} + \mu \begin{pmatrix} 1 \\ 0 \end{pmatrix}, & \text{for } x > 0, \end{cases} \quad (2)$$

where x and y are the new coordinates for which the border is along the line $x=0$, dividing the phase space into two halves L and R . μ is the new parameter, which is obtained by scaling ρ . τ_L and δ_L are the trace and determinant of the Jacobian matrix in side L . τ_R and δ_R are the corresponding values in side R . Since the trace and determinant are invariant under change of coordinates, these quantities are the same as in map f , calculated in the neighborhood of the point where border collision occurs. As the parameter μ is varied through zero, local bifurcations depend only on the values of τ_L , δ_L , τ_R , and δ_R appearing in (2) and therefore it suffices to study the bifurcations in the normal form (2) in exploring the border collision bifurcations in the piecewise smooth map (1).

The fixed points of the system in the two sides are given by

$$\begin{aligned} L^* &= \left(\frac{\mu}{1 - \tau_L + \delta_L}, \frac{-\delta_L \mu}{1 - \tau_L + \delta_L} \right) \\ R^* &= \left(\frac{\mu}{1 - \tau_R + \delta_R}, \frac{-\delta_R \mu}{1 - \tau_R + \delta_R} \right) \end{aligned}$$

and their stability is determined by the eigenvalues $\lambda_{1,2} = \frac{1}{2}(\tau \pm \sqrt{\tau^2 - 4\delta})$.

It may be noted that if

$$\tau_L > (1 + \delta_L) \quad \text{and} \quad \tau_R < (1 + \delta_R) \quad (3)$$

then there is no fixed point for $\mu < 0$ and there are two fixed points, one each in L and R , for $\mu > 0$. The two fixed points are born on the border at $\mu = 0$. We call this a *border collision pair* bifurcation. An analogous situation occurs if $\tau_L < (1 + \delta_L)$ and $\tau_R > (1 + \delta_R)$ as μ is reduced through zero. Due to symmetry of the two cases, we consider only the parameter region (3).

If $(1 + \delta_R) > \tau_R > -(1 + \delta_R)$ then for $\mu > 0$, the fixed point in L is a regular saddle and the one in R is an attractor. This is like a saddle-node bifurcation occurring on the border. Since this region in the parameter space always has a periodic attractor for $\mu > 0$, we exclude this region from our analysis when looking for chaotic behavior. The condition $\tau_R = -(1 + \delta_R)$, results in a nongeneric situation where all points on the line joining the points $(\frac{\mu}{1+\delta_R}, 0)$ and $(0, -\frac{\delta_R\mu}{1+\delta_R})$ are fixed points of the second iterate. We therefore concentrate on the parameter space region

$$\tau_L > (1 + \delta_L) \quad \text{and} \quad \tau_R < -(1 + \delta_R) \quad (4)$$

and investigate the property of the attractor for $\mu > 0$. We first consider the case $1 > \delta_L \geq 0$ and $1 > \delta_R \geq 0$.

For (4), L^* is a regular saddle and R^* is a flip saddle. Let \mathbf{U}_L and \mathbf{S}_L be the unstable and stable manifold of L^* and \mathbf{U}_R and \mathbf{S}_R be the unstable and stable manifold of R^* respectively. For (2), all intersections of the unstable manifolds with $x = 0$ map to the line $y = 0$. Since one linear map changes to another linear map across the $x = 0$ line, \mathbf{U}_L and \mathbf{U}_R experience folds along the x-axis. And all images of fold points will be fold points. By a similar argument we conclude that \mathbf{S}_L and \mathbf{S}_R fold along the y-axis, and all pre-images of fold points are fold points.

Let λ_{1L} , λ_{2L} be the eigenvalues in side L and λ_{1R} , λ_{2R} be the eigenvalues at side R . For condition (4), $\lambda_{1L} > \lambda_{2L} > 0$ and $0 > \lambda_{1R} > \lambda_{2R}$. The stable eigenvector at R^* has a slope $m_1 = (-\delta_R/\lambda_{1R})$ and the unstable eigenvector has a slope $m_2 = (-\delta_R/\lambda_{2R})$. Since points on an eigenvector map to points on the same eigenvector and since points on the y-axis map to the x-axis, we conclude that points of \mathbf{U}_R to the left of y-axis map to points above x-axis. From this we find that \mathbf{U}_R has an angle $m_3 = \frac{\delta_L \lambda_{2R}}{\delta_R - \tau_L \lambda_{2R}}$ after the first fold. Under condition (4) we have $m_1 > m_2 > 0$ and $m_3 < 0$. Therefore there must be a transverse homoclinic intersection in R . This implies an infinity of homoclinic intersections and the existence of a chaotic orbit.

We now investigate the stability of this orbit. The basin boundary is formed by \mathbf{S}_L . \mathbf{S}_L folds at the y-axis and intersects the x-axis at point C . The portion of \mathbf{U}_L to the left of L^* goes to infinity and the portion to the right of L^* leads to the chaotic orbit. \mathbf{U}_L meets the x-axis at point D , and then undergoes repeated foldings leading to an intricately folded compact structure as shown in Fig.3.

The unstable eigenvector at L^* has a negative slope given by $(-\delta_L/\lambda_{1L})$. Therefore it must have a heteroclinic intersection with \mathbf{S}_R . Since both \mathbf{U}_L and \mathbf{U}_R have transverse intersections with \mathbf{S}_R , by the Lambda Lemma [9] we conclude that for each point q on \mathbf{U}_R and for each ϵ -neighborhood $N_\epsilon(q)$, there exist points of \mathbf{U}_L in $N_\epsilon(q)$. Since \mathbf{U}_L comes arbitrarily close to \mathbf{U}_R , the attractor must span \mathbf{U}_L in one side of the heteroclinic point.

Since all initial conditions in L converge on \mathbf{U}_L and all initial conditions in R converge on \mathbf{U}_R , and since there

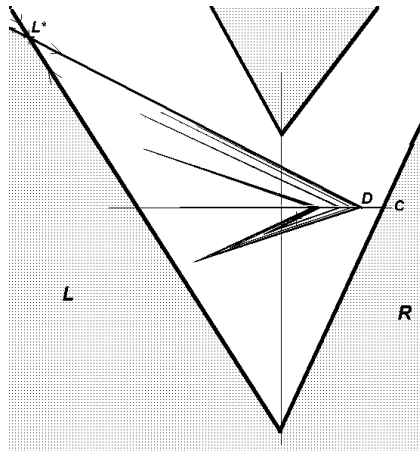


Figure 3: The stable and unstable manifolds of L^* for $\tau_L = 1.7$, $\delta_L = 0.5$, $\tau_R = -1.7$, $\delta_R = 0.5$. R^* is marked by the small cross inside the attractor.

are points of \mathbf{U}_L in every neighborhood of \mathbf{U}_R , we conclude that the attractor is unique. This chaotic attractor can not be destroyed by small changes in the parameters. Since small changes in the parameters can only cause small changes in the Lyapunov exponents, where the chaotic attractor is stable, it is also robust.

It is clear from the above geometrical structure that no point of the attractor can be to the right of point D . If D lies towards the left of C , the chaotic orbit is stable. If D falls outside the basin of attraction, it is an unstable chaotic orbit or chaotic saddle. From this, the condition of stability of the chaotic attractor is obtained as

$$\delta_L \tau_R \lambda_{1L} - \delta_R \lambda_{1L} \lambda_{2L} + \delta_R \lambda_{2L} - \delta_L \tau_R + \tau_L \delta_L - \delta_L^2 - \lambda_{2L} \delta_L > 0 \quad (5)$$

If $\delta_L = \delta_R = \delta$ this condition reduces to $\tau_R \lambda_{1L} - \lambda_{1L} \lambda_{2L} + \tau_L - \tau_R - \delta > 0$.

The robust chaotic orbit continues to exist as τ_L is reduced below $(1 + \delta_L)$. With τ_L slightly below $(1 + \delta_L)$, there is no fixed point in L for $\mu > 0$ but the invariant manifolds suffer only slight change. The invariant manifold of L associated with λ_{1L} still forms the attractor. The invariant manifolds in L , however, cease to exist for $\tau_L < 2\sqrt{\delta_L}$ since the eigenvalues become complex. As τ_L is reduced below $2\sqrt{\delta_L}$ there is a sudden reduction in the size of the attractor as it spans only \mathbf{U}_R . So long as \mathbf{U}_L exists, multiple attractors can not exist and therefore if the main attractor is chaotic, it is also robust.

Therefore we see that for $1 > \delta_L > 0$, $1 > \delta_R > 0$, the normal form (2) exhibits robust chaos in a portion of parameter space bounded by the conditions $\tau_R = -(1 + \delta_R)$, $\tau_L > 2\sqrt{\delta_L}$ and (5), as shown in Fig.4. There is a symmetric region of the parameter space with the roles of R and L interchanged, where the same phenomena are observed for $\mu < 0$.

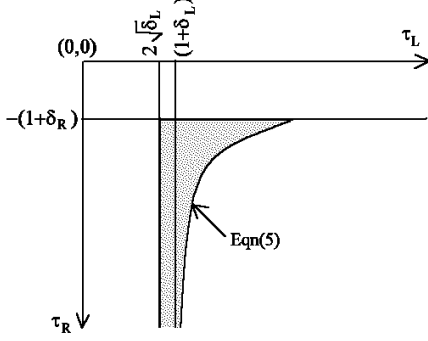


Figure 4: Schematic diagram of the parameter space region of the normal form (2) where robust chaos is observed for $1 > \delta_L > 0$, $1 > \delta_R > 0$ and $\mu > 0$.

At very low values of the determinant, i.e., when the system is very close to being one-dimensional, the main attractor may not remain chaotic even for $\tau_L > 2\sqrt{\delta_L}$, as periodic orbits become stable. The conditions for emergence of periodic windows for the one-dimensional case have been derived in [8, 10]. Therefore for one dimensional systems, the parameter range for robust chaos is bounded by $\tau_R = 1$, $\tau_R > -\frac{\tau_L}{\tau_L - 1}$, and the lower limit of τ_L is given by the conditions of existence of various periodic windows. Here the τ 's are to be interpreted as the slopes of the piecewise linear function in the two halves separated by $x = 0$. On the other hand, if the determinants in the two sides are unity, the region in the $\tau_L - \tau_R$ space for robust chaos shrinks to zero area.

The cases with negative determinant are investigated following the same method. For the sake of brevity, we present the results without much explanation.

For $-1 < \delta_R < 0$, we have $1 > \lambda_{1R} > 0$, $\lambda_{2R} < -1$, and R^* is located above the x-axis. A positive value of λ_{1R} implies that \mathbf{U}_L converges on \mathbf{U}_R from one side. If

$$\frac{\lambda_{1L} - 1}{\tau_L - 1 - \delta_L} > \frac{\lambda_{2R} - 1}{\tau_R - 1 - \delta_R} \quad (6)$$

then the intersection of \mathbf{U}_L with the x-axis remains the rightmost point of the attractor and (5) still gives the parameter range for boundary crisis. But if (6) is not satisfied, the intersection of \mathbf{U}_R with the x-axis becomes the rightmost point of the attractor, and the condition of existence of the chaotic attractor changes to

$$\frac{\lambda_{2R} - 1}{\tau_R - 1 - \delta_R} < \frac{\delta_L (\tau_L - \delta_L - \lambda_{2L})}{(\tau_L - 1 - \delta_L) (\delta_R \lambda_{2L} - \delta_L \tau_R)} \quad (7)$$

For $\delta_L < 0$ and $\delta_R < 0$, L^* is below the x-axis and the same logic as above applies. But if $\delta_L < 0$ and $\delta_R > 0$, the stable manifold of R^* has a negative eigenvalue and hence \mathbf{U}_L does not approach \mathbf{U}_R from one side. Therefore, if (6) is not satisfied, there is no analytic condition for boundary crisis — it has to be determined numerically.

For $\delta_L < 0$, the invariant manifolds \mathbf{U}_L and \mathbf{S}_L always exist as the eigenvalues are real for all τ_L . Therefore multiple attractors can not exist for $\delta_L < 0$.

Since (2) is a normal form of the piecewise smooth map (1), it is expected that robust chaos would be observable in many piecewise smooth maps in the neighborhood of border collision bifurcations, provided that there are no more than one period-1 fixed point in R_a and R_b , there exist homoclinic as well as heteroclinic intersections of the invariant manifolds associated with these fixed points, and the trace and determinant at the two sides of the border-line satisfy the above conditions. The example of the boost converter is a case in point.

A major conclusion of this Letter is that one should use piecewise smooth systems in applications that require reliable operation under chaos.

* Electronic address: soumitro@ee.iitkgp.ernet.in

† Electronic address: yorke@ipst.umd.edu

‡ Also with the Institute for Plasma Research and Department of Mathematics, University of Maryland, College Park, USA. Electronic address: grebogi@chaos.umd.edu

References

- [1] S. Hayes, C. Grebogi and E. Ott, Phys. Rev. Lett. **70**, 3031 (1993).
- [2] J. M. Ottino, *The Kinematics of Mixing: Stretching, Chaos and Transport*, (Cambridge Univ. Press, 1989).
- [3] S. H. Isabelle, G. C. Verghese, and S. Venkataraman, To appear in *IEEE Trans. Circuits & Systems-I*.
- [4] J. H. B. Deane and D. C. Hamill, *Electronics Letters*, **32**, 1045 (1996).
- [5] J. Graczyk and G. Świątek, *Annals Math.* **146**, 1 (1997).
- [6] E. H. Nusse and J. A. Yorke, *Physica D*, **57**, 39 (1992).
- [7] E. H. Nusse, E. Ott, and J. A. Yorke, *Phys. Rev. E*, **49**, 1073 (1994).
- [8] E. H. Nusse and J. A. Yorke, *Int. J. Bifurcation chaos Appl. Sci. Eng.*, **5**, 189 (1995).
- [9] K. T. Alligood, T. D. Sauer, and J. A. Yorke, *Chaos: An Introduction to Dynamical Systems*, (Springer, 1996).
- [10] Y. L. Maistrenko, V. L. Maistrenko, and L. O. Chua, *Int. J. Bifurcation Chaos Appl. Sci. Eng.*, **3**, 1573 (1993).